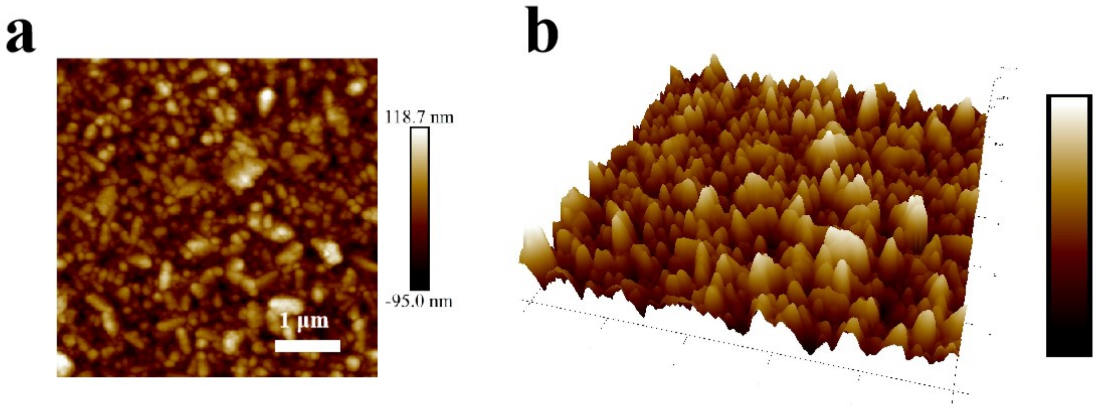

Fig. S1. (a, b) AFM images of the $[PEI/P_2W_{18}]_{20}$ film for 3D and 2D images.

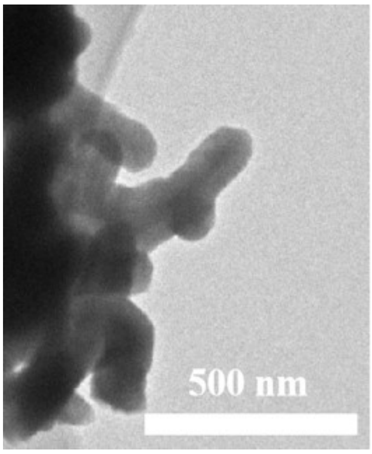

Fig. S2. The TEM image of the $W_{18}O_{49}/[PEI/P_2W_{18}]_{20}$ film after 500 stability cycles.

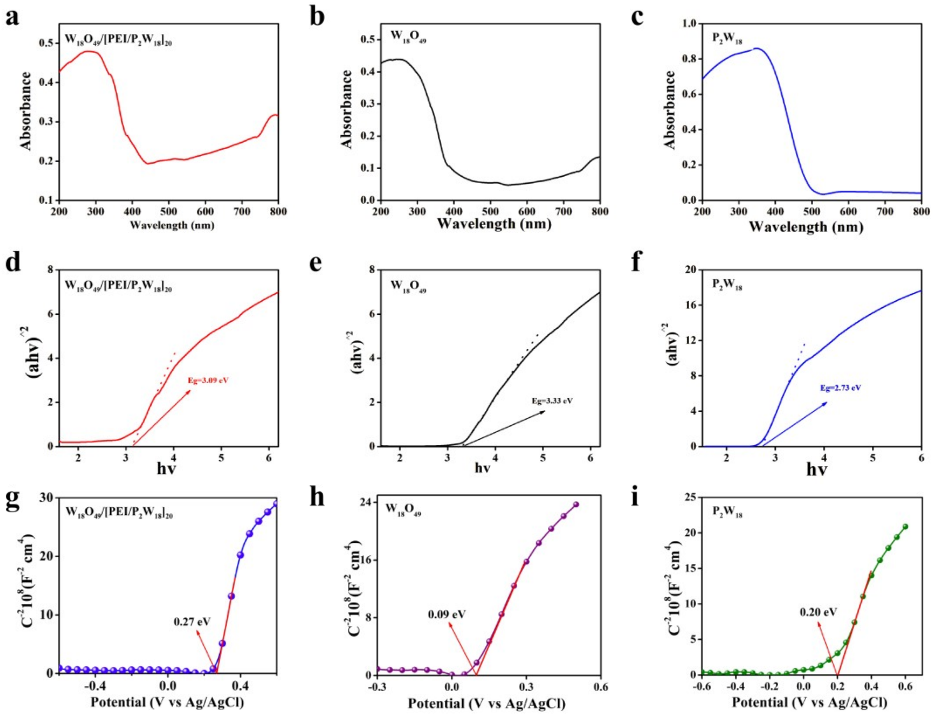

Fig S3. (a-c) UV-VIS diffuse reflectance spectra of the $W_{18}O_{49}$/[PEI/P_2W_{18}]$_{20}$, $W_{18}O_{49}$ and P_2W_{18} film. (d-f) Calculated band gaps of the $W_{18}O_{49}$/[PEI/P_2W_{18}]$_{20}$, $W_{18}O_{49}$ and P_2W_{18} film after converting the spectra to the Kubelka-Munk plot. Mott-Schottky plots of the (g) $W_{18}O_{49}$/[PEI/P_2W_{18}]$_{20}$ film, (h) $W_{18}O_{49}$ film and (i) P_2W_{18} film.

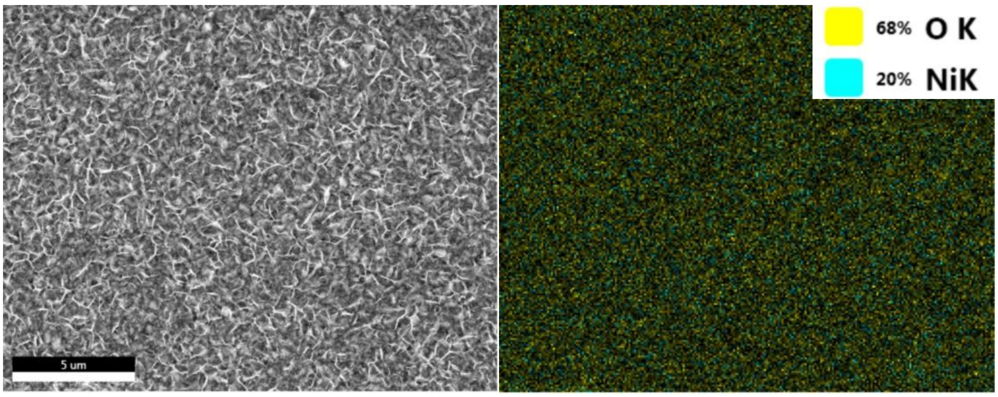

Fig. S4. SEM diagram of NiO and corresponding EDS diagram.

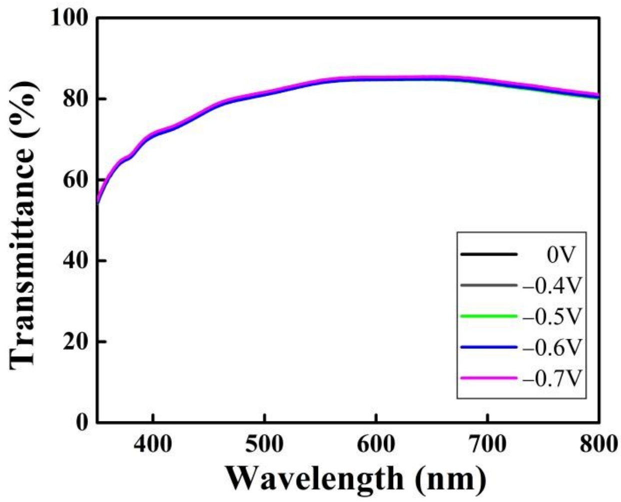

Fig. S5. The transmittance curve of NiO film at 0 V, − 0.4 V ~ − 0.7 V in the wavelength range of 350−800 nm.

Table S1 Comparison of electrochromic and energy storage performance in this work and previous works about POMs-based and inorganic metal oxides electrodes.

EC material	Specific capacitance	Coloration efficiency (cm^2/C)	Transmittance contrast	Switching speed (color / bleach (s))	Ref.
$WO_{2.72}/P_2W_{18}$	**30.45 mF cm^{-2}**	**224.15**	**ΔA = 2.00 at 650 nm**	**3.92/0.75**	**This work**
WO_{3-x} (amorphous)	-	125–80	56–70% at 550–800 nm	5 s/2.5 s	1–4
$WO_{2.72}$ assembled on Ag nanowires	-	35.7	58–86% at 550 nm	2 s/4 s	5
$WO_{2.72}/P_8W_{48}$	-	42.31	64% at 630 nm and 88% at 915 nm	26/86	6
MoO_3–WO_3/Ag/MoO_3–WO_3	-	70	72.9 – 79.3 at 400 – 800 nm	2.7/4.1	7
$W_{2.72}$ nanowire	-	82.1	68.7% at 633 nm	2.3/1.4	8
NW-P_2W_{18}	-	69.0	45.1 at 650 nm	1.9/6.7	9
WO_3-V_2O_5	38.75 mF cm^{-2}	61.5	60 at 700 nm	4.9/0.61	10
Ag NWs/WO_3	13.6 mF cm^{-2}	80.2	44.1 at 633 nm	1.7/1.0	11
h-WO_3/TiO_2 NRAs	10.93 mF cm^{-2}	69.2	73.45 at 633 nm	6.6/2.0	12
TiO_2 PANI	3.6 mF cm^{-2}	78	76.9 at 600 nm	3.6/3.3	13
P_5W_{30}/PAH-Fe(phen)$_3$	10.45 mF cm^{-2}	94.73	35.17 at 650 nm	2.49/0.9	14
NW/P_2W_{17}/Fe(phen)$_3$	135.8 F cm^{-3}	194.5	34.3 at 600 nm	2.8/6.2	15
Hybrid WO_3 nanoarrays	47.4 mF cm^{-2}	92.3	-	3.0/3.6	16

[1] C. Guille´n and J. Herrero, J. Mater. Sci. Technol., 2021, 78, 223–228.

[2] H. Yu, J. Guo, C. Wang, J. Zhang, J. Liu, X. Zhong, G. Dong and X. Diao, Electrochim. Acta, 2019, 318, 644–650.

[3] R. Baetens, B. P. Jelle and A. Gustavsen, Sol. Energy Mater. Sol. Cells, 2010, 94, 87–105.

[4] T. V. Nguyen, K. A. Huynh, Q. V. Le, H. Kim, S. H. Ahn and S. Y. Kim, Int. J. Energy Res., 2021, 45, 8061–8072.

[5] J. Wang, Y. Lu, H. Li, J. Liu and S. Yu, J. Am. Chem. Soc., 2017, 139, 9921–9926.

[6] H. Gu, C. Guo, S. Zhang, L. Bi, T. Li, T. Sun and S. Liu, ACS Nano, 2018, 12, 559–567.

[7] W. Dong, Y. Lv, L. Xiao, Y. Fan, N. Zhang and X. Liu, ACS Appl. Mater. Interfaces, 2016, 8, 33842–33847.

[8] J. L. Xie, B. Song, G. L. Zhao and G. R. Han. Appl. Phys. Lett. 2018, 112, 231902.

[9] S. P. Liu, X. S. Qu, Appl. Surf. Sci. 2017, 184,129–195.

[10] A. K. Prasad, J. Y. Park, S. H. Kang, K. S. Ahn, Electrochim. Acta. 2022, 422, 140340.
[11] L.X. Shen, L.H. Du, S.Z. Tan, Z.G. Zang, C.X. Zhao, W.J. Mai, Chem. Commun. 52 (2016) 6296–6299.
[12] L.L. Zhao, X.H. Huang, G.H. Lin, Y.Q. Peng, J. Chao, L.Z. Yi, X.X. Huang, C. Li, W.B. Liao, Chem. Eng. J. 420 (2021) 129871.
[13] S.Y. Zhang, P.Y. Lei, J.J. Fu, X.R. Tong, Z.P. Wang, G.F. Cai, Appl. Surf. Sci. 607 (2023) 155015.
[14] S. P. Liu, J. Zhang, Y. Y. Song, S. Y. Feng, Y. Y. Yang, X. S. Qu, Eur. J. of Inorg. Chem. 2022, e202200543.
[15] D. X. Chu, X. S. Qu, S. F. Zhang, J. R. Zhang, Y. Y. Yang, W. J. An, New J. Chem. 2021, 45, 19977–19985.
[16] Y. D. Shi, M. J. Sun, Y. Zhang, J. W. Cui, Y. Q. Wu, H. H. Ta, J. Q. Liu and Y. C. Wu, Sol. Energy Mater. Sol. Cells. 2020, 212, 110579.